Astronomy & Astrophysics manuscript no. article
January 17, 2017
©ESO 2017

The distribution of stars around the Milky Way's black hole

III. Comparison with simulations

H. Baumgardt[1], P. Amaro-Seoane[2], and R. Schödel[3]

[1] School of Mathematics and Physics, University of Queensland, St. Lucia, QLD 4072, Australia e-mail: h.baumgardt@uq.edu.au
[2] Institut de Ciències de l'Espai (CSIC-IEEC) at Campus UAB, Carrer de Can Magrans s/n 08193 Barcelona, Spain
Institute of Applied Mathematics, Academy of Mathematics and Systems Science, Chinese Academy of Sciences, Beijing 100190, China
Kavli Institute for Astronomy and Astrophysics, Beijing 100871, China
Zentrum für Astronomie und Astrophysik, TU Berlin, Hardenbergstraße 36, 10623 Berlin, Germany
e-mail: pau@ice.cat
[3] Instituto de Astrofísica de Analucía, Glorieta de la Astronomía s/n, 18008 Granada, Spain

draft January 17, 2017

ABSTRACT

Context. The distribution of stars around a massive black hole (MBH) has been addressed in stellar dynamics for the last four decades by a number of authors. Due to its proximity, the centre of the Milky Way is the only observational test case where the stellar distribution can be accurately tested. Past observational work indicated that the brightest giants in the Galactic Centre (GC) may show a density deficit around the central black hole, not a cusp-like distribution, while we theoretically expect the presence of a stellar cusp.
Aims. In this work we present a solution to this long-standing problem.
Methods. We perform direct-summation $N-$body simulations of star clusters around massive black holes and compare the results of our simulations with new observational data of the GC's nuclear cluster.
Results. We find that after a Hubble time, the distribution of bright stars as well as the diffuse light follow power-law distributions in projection with slopes of $\Gamma \approx -0.3$ in our simulations. This is in excellent agreement with what is seen in star counts and in the distribution of the diffuse stellar light extracted from adaptive optics (AO) assisted near infrared observations of the GC.
Conclusions. Our simulations also confirm that there exists a missing giant star population within a projected radius of a few arcsec around Sgr A*. Such a depletion of giant stars in the innermost 0.1 pc could be explained by a previously present gaseous disc and collisions, which means that a stellar cusp would also be present at the innermost radii, but in the form of degenerate compact cores.

Key words. Galaxy: centre – Galaxy: kinematics and dynamics – Galaxy: nucleus

arXiv:1701.03818v1 [astro-ph.GA] 13 Jan 2017

1. Introduction

The Galactic centre (GC) is the closest nucleus to us, offering the unique possibility to study the interaction between a supermassive black hole (SMBH) and its surrounding star cluster using individual, resolved stars. Adaptive Optics (AO)-assisted near-infrared photometric and spectroscopic studies of the stars within about 1 pc of the SMBH have shown that the surface density of massive, young type stars is rising steeply towards Sagittarius A* (Sgr A*, the electromagnetic manifestation of the SMBH) while the density distribution of bright, late type stars down to the apparent median luminosity of the Red Clump ($K_s \approx 15.5$) – and therefore mostly old and lower mass stars – rises much more slowly and may even be flat within a few 0.1 pc of the black hole (Schödel et al. 2007; Do et al. 2009).

Typically, the projected stellar surface number density (and equivalently the 3D density) is described by a power-law of the form $\Sigma(R) \propto R^{\Gamma}$, where R is the distance from Sgr A*. Buchholz et al. (2009) for example found that the surface density distribution within a projected radius $R = 6$" of Sgr A* can be described with an exponent $\Gamma = -0.2 \pm 0.1$, which would correspond to a decreasing density within the innermost few arcseconds (one arcscond corresponds to approximately 0.04 pc at the distance of the GC).

Since the relaxation time at the GC is of order of a Hubble time, old stars should have had enough time to settle into an equilibrium distribution around the black hole. Bahcall & Wolf (1976) found that a single-mass stellar population should settle into a power-law cusp with 3D slope of $\Gamma = -1.75$ within the influence radius of the central supermassive black hole, much steeper than what is observed. This has led to the so called 'missing giant star' problem. Moreover, the impact goes beyond stellar dynamics and the Galactic Centre, because these massive stars close to the MBH are the precursors of compact objects, which might eventually become a source of gravitational waves for a space-borne observatory such as LISA or Taiji (Amaro-Seoane et al. 2013, 2012; Gong et al. 2015). The gradual inspiral of a stellar-mass black hole has been coined as an "extreme-mass ratio inspiral", and accumulates hundreds of thousands of cycles in the detector band, with impressive implications in fundamental physics and astrophysics (Amaro-Seoane et al. 2007; Amaro-Seoane 2012; Amaro-Seoane et al. 2015).

A number of works have tried to explain this conundrum with different ideas, which follow one of three possibilities: When Genzel et al. (1996) first discovered missing RGB stars, they proposed that this can be due to stellar collisions depleting giant stars in the innermost parts due to the high stellar densities that are reached near the SMBH. Later, Davies et al. (1998),

Alexander (1999), Bailey & Davies (1999) and Dale et al. (2009) addressed this idea in detail and came to the conclusion that it can only explain the absence of the brightest and most extended giant stars. A different suggested possibility to explain the missing stars is that our GC does not only have one, but a binary of two massive black holes. This hypothesised binary could indeed carve a core into the stellar distribution due to three-body interactions, as shown by a number of authors (Baumgardt et al. 2006; Portegies Zwart et al. 2006; Matsubayashi et al. 2007; Löckmann & Baumgardt 2008; Gualandris & Merritt 2012). Nonetheless, the mass of the secondary needs to be of the order of $\sim 10^5\ M_\odot$ to explain the observed core. Such a massive secondary black hole would require that the Milky Way relatively recently went through a major merger, which is excluded by observations (see Hansen & Milosavljević 2003; Yu & Tremaine 2003; Chen & Liu 2013). Also, the existence of such a massive secondary black hole is largely ruled out from a number of other considerations, e.g. constraints on the proper motion of Sgr A* from radio interferometry (see Gualandris & Merritt 2009). A number of inspiraling smaller-mass black holes could also carve out the observed core, which would relax the major merger requirement, but to our knowledge this interesting possibility has not been explored yet. It has also been put forward that a star cluster falling towards the GC could increase the density profile outside of $10''$, so that within that distance the profile would be like a core (Kim & Morris 2003; Ernst et al. 2009; Antonini et al. 2012). However, mass segregation would rebuild a steeper profile in as fast as a quarter of the relaxation time (as shown by Preto & Amaro-Seoane 2010a; Amaro-Seoane & Preto 2011). This requirement would hence need a steady inflow of clusters about every 10^7 years to repeatedly wipe out the cusp. Finally, Merritt (2010) suggested that if the nuclear cluster in the galactic centre formed with a large enough initial core radius, the current stellar distribution could still have a central core. While this solution is possible, it requires fine tuning in the initial conditions to produce the density distribution seen in the Galactic Centre. Amaro-Seoane & Chen (2014) proposed that the stellar disc we observe at the Galactic Centre is connected to the missing bright giants: The precursor gaseous disc must have gone through a fragmentation phase, which produced dense enough clumps to ensure an efficient removal of the outer layers of the giants via collisions, rendering them invisible to observations. Their degenerate cores would nonetheless populate the same area of phase space were the missing bright giants should be. Their analytical work has been later confirmed with dedicated and detailed numerical simulations (Kieffer & Bogdanović 2016).

Due to the extreme extinction and source crowding toward the GC, observational studies are complex, even with the power of AO-assisted 10m-class telescopes. In particular, the spectroscopic identification of stars is limited to bright giants and massive, young stars, while the crowding makes it almost impossible to detect main-sequence stars with less than two solar masses. Gallego Cano et al. (2017) and Schödel et al. (2017) have revisited the observational data with improved methodologies. On the one hand, they could push the completeness of the star counts one magnitude deeper than in previous studies. This means that not only bright giants down to the Red Clump (RC), but also fainter giants and sub-giants are included in the star counts. Thus we now have access to two stellar tracer populations, with different luminosities but similar masses, that can provide us with information on the structure of the nuclear star cluster (NSC). On the other hand, they also succeeded in deriving the surface brightness profile of the diffuse stellar light, which traces even fainter stars, probably sub-giants and main sequence stars of $\lesssim 1.5\,\mathrm{M}_\odot$. Both new analyses provide fully consistent results: The projected stellar density can be described by a power-law with an exponent of $\Gamma \approx -0.35$ for three different tracers: (sub-)giants in the magnitude ranges $16.5 \leq K_s \leq 17.5$ and $17.5 \leq K_s \leq 18.5$ and the diffuse light, which is created mainly by sub-giants and main sequence stars. After combining the data on the central 1-2 pc with other measurements of the stellar distribution on scales 2-10 pc, the authors de-project the surface density and determine a 3D power law index of $\Gamma \approx -1.2$. As concerns Red Clump stars and brighter giants, Schödel et al. (2017) reproduce the findings of previous work, i.e. a flattening of the stellar density distribution in the innermost 0.1 to 0.3 pc. They conclude that outside of this projected radius, the distribution of these stars is consistent with a stellar cusp, but that some process has probably altered the giant stars' distribution at smaller radii.

The masses of all tracer populations are very similar, between $1 - 2\ \mathrm{M}_\odot$. Such stars can live for several Gyr and thus be old enough to be dynamically relaxed. If the faint stars and diffuse stellar light at the GC indeed trace an underlying old stellar population (of age $\sim 10^9$ to $\sim 10^{10}$ years) then the stellar cusp is surprisingly shallow. Here it becomes important to look at the theory in more detail. The steep power-law cusp solution found by Bahcall & Wolf (1976) only holds for a single-mass stellar population. If stars follow a distribution of masses, mass segregation causes stars of different masses to follow different density distributions with more massive components having steeper central slopes (Bahcall & Wolf 1977; Baumgardt et al. 2004; Amaro-Seoane et al. 2004; Freitag et al. 2006). In particular, Alexander & Hopman (2009) and Preto & Amaro-Seoane (2010b) independently derived the so-called "strong-mass segregation" solution for two-stellar mass groups, which is more efficient than one expected from the theory of Bahcall & Wolf (1977), which is mathematically correct but physically inappropriate because of the number fractions they used.

Baumgardt et al. (2005) showed that in globular clusters containing intermediate-mass black holes, the surface density distribution of luminous stars can be described by a weak power-law cusp distribution, offering a new way to explain the missing mass problem seen in the GC. However, their results cannot directly be applied to it, since in their simulations all stars formed at the same time, which is a good approximation for a globular cluster, but not for the nuclear cluster at the centre of the Milky Way where stars have formed continuously over a Hubble time (Pfuhl et al. 2011). In addition, while the GC has a relaxation time of the same order as its age, the star clusters in their simulations were simulated for about 10 relaxation times.

In this paper we present results of direct N-body simulations aimed at studying the dynamics of the nuclear cluster in the Milky Way. In our simulations, we evolve a star cluster surrounding a central massive black hole over a Hubble time under the combined influence of two-body relaxation and continuous star formation. Our paper is organised as follows: In section 2 we discuss our simulations and in section 3 we compare the resulting distribution of stars with observations of the nuclear star cluster in the Galactic centre. Sec. 4 presents our conclusions.

2. The simulations

We have run collisional $N-$body simulations of star clusters containing massive central black holes using the GPU enabled version of the collisional N-body code *NBODY6* (Aarseth 1999; Nitadori & Aarseth 2012). The stellar mass distribution was given by a Kroupa (2001) mass function with lower and upper mass

limits of 0.1 and 100 $M_\odot$ respectively. Such a mass function is compatible with observations of the mass-to-light ratio of the nuclear cluster and the temperature and luminosity distribution of individual giant stars in the nuclear cluster (Löckmann et al. 2010; Pfuhl et al. 2015). Due to the high escape velocity from the nuclear cluster, we assumed a 100% retention fraction for stellar-mass black holes and neutron stars upon their formation. We also assumed solar metallicity for the stars in our simulation, which is compatible with the average metallicity of stars in the galactic centre (Ryde & Schultheis 2015; Do et al. 2015).

In our simulations, we added new stars to the clusters during the simulations and followed the evolution of the star clusters under the combined influence of star formation, stellar evolution and two-body relaxation. Pfuhl et al. (2011) found that most stars in the nuclear cluster are old, with about 80% of them having been born more than 5 Gyr ago. They also found that an exponentially decreasing star formation rate according to

$$SFR(t) = e^{-t/\tau_{SFR}} \quad (1)$$

with a characteristic timescale $\tau_{SFR} = 5.5$ Gyr matches the age distribution of old stars in the nuclear cluster. We therefore started our simulations with a star cluster containing $N = 50,000$ stars and an MBH that contained 15% of the cluster mass, similar to the mass ratio seen for the galactic centre SMBH (see e.g. Genzel et al. 2010, and references therein). We then simulated the evolution of this cluster for 1 Gyr and added new stars to it after 1 Gyr with a rate given by eq. 1. We evolved the new cluster for another Gyr before adding the next generation of stars and repeated this process until the cluster reached an age of $T = 13$ Gyr. Throughout the evolution, the mass ratio between the cluster and the central MBH was kept constant at 15%, i.e. we assumed that the MBH is growing at the same rate as the nuclear cluster. The new stars added to the simulation followed a King (1966) model with dimensionless central potential of $W_0 = 5.0$ initially. In order to study the influence of the initial density profile on the final results we also ran simulations in which the initial density profiles had central potentials of $W_0 = 3.0$ and $W_0 = 7.0$, but found that the final slopes of the power-law profiles do not change by more than $\Delta\Gamma = \pm 0.1$ in surface density, confirming that the galactic centre nuclear star cluster is dynamically relaxed. When setting up the King (1966) models, we took the potential of the central black hole into account when calculating the stellar velocities. After 13 Gyr, we ended up with star clusters containing about $\sim 255,000$ stars and a final mass of $M_C = 9.5 \cdot 10^4$ $M_\odot$.

The nuclear cluster in the galactic center has a projected half-light radius of $R_{hNC} = 4.2 \pm 0.4$ pc and a mass of $M_{NC} = 2.5 \pm 0.4 \cdot 10^7$ $M_\odot$ (Schödel et al. 2014). Using the definition of the half-mass relaxation time as given by Spitzer (1987) and assuming the 2D half-light radius to be 75% of the 3D one, this results in a half-light relaxation time of $T_{RH} \approx 14$ Gyr. We therefore use an initial half-mass radius of our simulated clusters of $r_{hSim} = r_{hNC} \cdot (M_{Sim}/M_{NC})^{1/3} = 26.9$ pc, so that our simulated clusters have the same half-mass relaxation time as the nuclear cluster and evolve dynamically with the same rate per physical time. At the end of the simulations, we scaled our clusters down to a projected half-light radius of $R = 4.2$ pc, so that we can directly compare with observational data. In total we perform 3 realizations using different random number seeds for each density profile and overlay the results centered on the MBH after scaling each cluster to the same half-mass radius.

Fig. 1 depicts a J-K_S vs K_S colour-magnitude diagram of the stars in our simulation after $T = 13$ Gyr, calculated using the PARSEC isochrones (Bressan et al. 2012). In order to calculate the apparent K_S band magnitudes, we assume a distance of 8 kpc to the galactic centre and a K_S band extinction of $A_{K_S} = 2.54$ mag (Schödel et al. 2010) for all stars. The different generations of stars which were added to the star cluster during the simulation can clearly be distinguished in the CMD. In the following, we will use stars with $K_S < 19$ mag (shown in red) to compare with the number density profile of resolved stars from Gallego Cano et al. (2017). To compare with the diffuse light profile of Schödel et al. (2017), we use all stars fainter than this limit and sum up their K_S band luminosities. Using these limits, resolved stars have masses in the range $0.86 < m < 2.31$ $M_\odot$ while 90% of the diffuse light is created by stars with masses $0.78 < m < 1.76$ $M_\odot$. On average, the resolved stars are about 0.25 $M_\odot$ more massive than the brightest stars that contribute to the unresolved light.

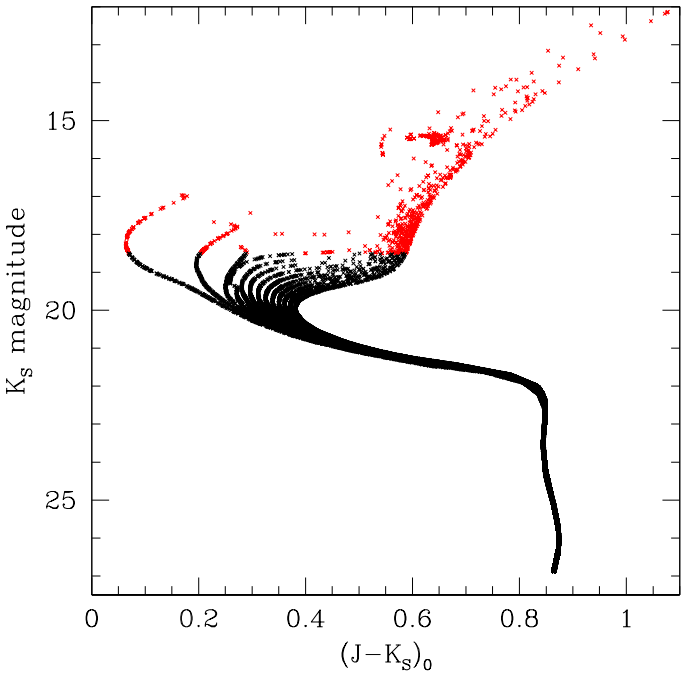

Fig. 1. $J - K_S$ colour magnitude diagram of the simulated nuclear clusters after 13 Gyr of evolution for a distance of 8 kpc to the Galactic centre and and an average reddening of $A_{K_S} = 2.54$ mag. The different stellar generations that were added to the simulations can clearly be distinguished in the CMD. Stars marked in red have $K_S < 19$ and are used to compare with the density profile of resolved stars from Gallego Cano et al. (2017). The remaining stars are used to create the diffuse light profile of the simulated clusters.

3. Results

Fig. 2 shows the density distribution of different types of stars after 13 Gyrs of evolution. Shown are the density distributions of stellar mass black holes, giant stars, which we assume to be all stars with K-band luminosities $K_S < 19$, upper main sequence stars with masses between 0.6 $M_\odot$ and 0.8 $M_\odot$ and lower main sequence stars with masses between 0.1 and 0.3 $M_\odot$. For clarity we have shifted all curves vertically to separate the different curves from each other. We also scaled the final cluster to have a projected half-light radius of 4.2 pc to match the galactic centre nuclear cluster. For this half-light radius the influence radius of the central black hole, i.e. the radius where the cumulated mass in stars becomes equal to the central black hole mass is $r_{BH} = 2.9$ pc. This value is close to the 3D break radius of $r \approx 3$ pc found

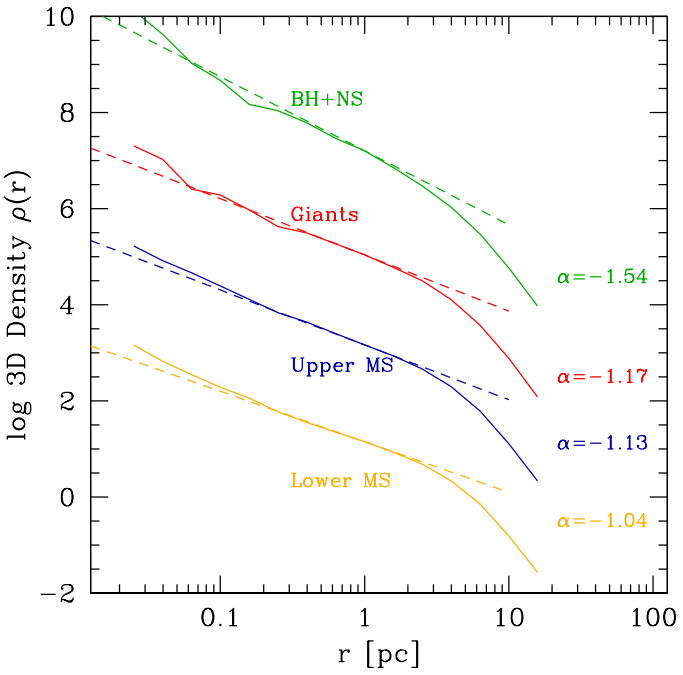

Fig. 2. Spatial density of different stellar components at the end of our simulations. From top to bottom, we show the density distribution of black holes and neutron stars (green), giant stars with apparent magnitudes $K_S < 18.5$ (red), upper main-sequence stars with masses 0.6 $M_\odot$ and 0.8 $M_\odot$ (blue) and low-mass main sequence stars with masses 0.1 and 0.3 $M_\odot$ (orange). For clarity, curves are shifted vertically. Dashed lines show power-law density distributions $\rho(r) \sim r^\Gamma$ fitted to the density distribution inside the influence radius of the black hole ($r_{BH} = 2.8$ pc). Due to mass segregation, the slope steepens from $\Gamma = -1.04$ for the lowest-mass main sequence stars to $\Gamma = -1.54$ for black holes.

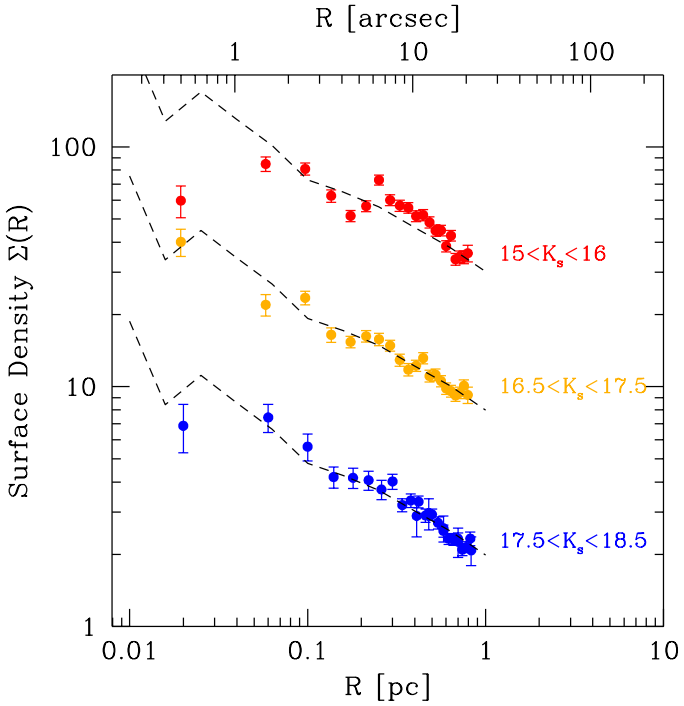

Fig. 3. Surface density $\Sigma(R)$ of old giant stars in the galactic centre for three different K_S band intervals. The data points are taken from the observations of Gallego Cano et al. (2017), while the dashed lines show the profile that we obtain for giant stars at the end of our simulations. It can be seen that the profiles are in excellent agreement with each other in the different magnitude intervals with the exception of the innermost density profile of stars in the magnitude interval $15 < K_S < 16$.

by Gallego Cano et al. (2017) and Schödel et al. (2017) by fitting Nuker profiles to the stellar density distributions in the Galactic centre.

It can be seen that inside the influence radius, the density distribution of the different stellar components can be well described by single-power law distributions. Black holes and neutron stars follow a power-law distribution with the steepest slope of $\Gamma = -1.54$, close to the theoretically predicted slope of $\Gamma = -1.75$ for a single-mass stellar population around a massive black hole (Bahcall & Wolf 1976). Due to mass segregation, all other components follow flatter density distributions. The slopes vary however by less between $\Delta\Gamma = 0.1$ between giant stars and the lowest-mass main sequence stars. Overall the power-law slopes of the different stellar mass groups are flatter than what Baumgardt et al. (2004) found for a single-age stellar cluster with the same initial mass function after $T = 12$ Gyr of evolution (see their Fig. 7). This indicates that the galactic centre star cluster is dynamically not yet completely relaxed due to its relatively long relaxation time ($T \sim 14$ Gyr). In addition, the continuous star formation reduces mass segregation between the different stellar components.

Due to the small amount of mass segregation, low mass stars dominate the stellar mass profile for all radii outside 0.01 pc and the luminosity profile closely follows the mass profile in the nuclear cluster, i.e. we do not predict a strong variation of the M/L profile of the nuclear cluster with radius. When scaled to the galactic centre, our simulations predict about ~ 300 stellar-mass black holes and a total mass of 7000 $M_\odot$ in stars inside the central 0.1 pc. Our mass estimate is in good agreement with the approximate 10^4 $M_\odot$ of total mass within this region that can be calculated with the Nuker model and the mass normalisations of Schödel et al. (2017) and also consistent with the upper limit of $1.3 \cdot 10^5$ $M_\odot$ recently derived by Boehle et al. (2016). We note that these mass limits have been derived assuming a mass-to-light ratio independent of radius for the nuclear star cluster.

Fig. 3 depicts the distribution of bright stars in the central parsec and compares it with the observed distribution of late-type giant stars within three different K_S-band intervals as determined by Gallego Cano et al. (2017). In order to avoid uncertainties and systematic biases in mixing different observational data sets, we only depict the NACO data, i.e. data in the radial range from 0.0011 pc to 1 pc in Fig. 3. In order to increase the statistical significance of our results, we use all stars with $K_S < 19$ to compare with the observed distribution in the three magnitude intervals. This is justified since the observed stars are giant stars, which show only a small dependence of average mass and age with luminosity. Hence we expect the stars in the different magnitude bands to follow similar density distributions in our simulations. It can be seen that the observed and simulated density profiles agree very well with each other. The combined surface density distribution of the three simulations we have performed can be fitted by a power-law distribution $\Sigma(R) \sim R^\Gamma$ with a slope $\Gamma \sim -0.39$ in the range 0.04 pc $< R <$ 0.8 pc. This is in excellent agreement with the observed density distributions of bright stars, which have best-fitting slopes of $\Gamma \sim -0.29$ for stars with $15 < K_S < 16$, $\Gamma = -0.39$ for stars with $16.5 < K_S < 17.5$ and $\Gamma = -0.45$ for stars with $17.5 < K_S < 18.5$ (Gallego Cano et al. 2017). The observed data has almost the same slopes in the different bands, as expected from our simulations. While we compare our results only to the most recent results, we note that pre-

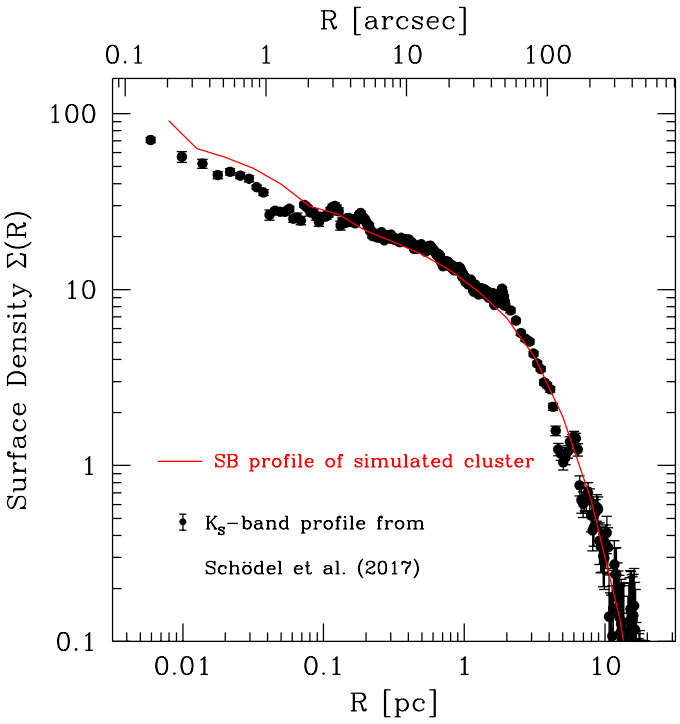

Fig. 4. K_S band surface luminosity profile $\Sigma(R)$ of the diffuse light of the galactic centre star cluster. The data points show the results of Schödel et al. (2017) corrected for differential extinction. The red line shows the surface density profile of the simulated cluster, determined from all main-sequence stars fainter than $K_S > 19$. Theoretical and observational profiles are in excellent agreement with each other outside the innermost few arcsec.

vious determinations of the surface density distribution of late-type giant stars (e.g. Schödel et al. 2007; Buchholz et al. 2009) are also compatible with our results, at least outside the central few arcsec. Stars with $15 < Ks < 16$ appear to display a density deficit inside the central ~ 0.1 pc, while their distribution at larger radii agrees with our simulations. This could indicate that some depletion process like giant star collisions or disc passages has altered their apparent distribution at the very center.

Fig. 4 compares the surface density profile of diffuse light in the galactic centre from Schödel et al. (2017) with the results of our simulations. The black data points depict the K_S band surface luminosity derived by Schödel et al. (2017) after correction for differential extinction. The red line shows the surface luminosity density of faint stars in our simulations. The simulated surface light distribution be well described by a single power-law profile with $\Sigma(R) \sim R^{-0.37}$ inside 0.5 pc, which is close to the observed profile which has $\Gamma = -0.28 \pm 0.03$ (Schödel et al. 2017). The fitted slope is nearly the same as in case of the resolved stars, again indicating that there was insufficient time for the nuclear cluster to develop significant mass segregation between main sequence stars of different masses. There is a clear steepening of the observed profile beyond 20 arcsec. This steepening is also present in the simulated data and is due to the steepening of the profile outside the influence radius of the central black hole. The surface density of the diffuse light may show some systematic uncertainties at radii R = 1-2" because of the presence of very bright stars and the related difficulty of accurate PSF subtraction in this region (see discussion in Schödel et al. 2017). We also see that our model somewhat over-predicts the surface density of diffuse light at radii $R < 2$". However, the qualitative agreement, in particular the slope of the power-law at larger radii is very good.

We conclude that the simulated and observed data agree excellently with each other. In particular the inferred power-law indices of the surface densities as well as the corresponding 3D power-law slopes (see caption of Fig. 2) agree well with the values estimated by Gallego Cano et al. (2017) and Schödel et al. (2017). The surface density profile of both resolved stars and diffuse light of the nuclear cluster are therefore entirely compatible what one should expect for a star cluster around a massive black hole that is evolving under the combined influence of dynamical relaxation and continuous star formation given the age and star formation history of the nuclear cluster.

Conclusions

The existence of stellar cusps in relaxed clusters around massive black holes is a long-standing prediction of theoretical stellar dynamics. Yet, it has escaped confirmation for decades for multiple reasons, some observational and some theoretical. On the observational side, there is only a single target where the cusp theory can be tested with current instrumentation: the Galactic Centre. Extragalactic nuclei are too far away for current instrumentation and the existence of (intermediate) massive black holes in globular clusters is still debated. However, the GC is not an easy target and both number counts and stellar classification suffer from the very high and spatially highly variable interstellar extinction as well as from the extreme source crowding. Observational evidence has therefore been ambiguous for a long time. Recent new analyses, however have found a stellar cusp around Sgr A*, with very consistent morphologies for different tracer populations which differ by several magnitudes in brightness. The cusp has been found to be rather shallow. This is one of the reasons why it has so successfully escaped detection over a long time.

On the theoretical side, the main limitation was probably that too simple systems were analysed. As we now know, the nuclear cluster around the SMBH at the GC is a highly complex system and has suffered many episodes of repeated star formation and/or cluster infall. This work presents a first attempt to take the complex star formation history of the Milky Way's NSC into account. As we have shown, two-body relaxation and repeated star formation across the lifetime of the Galaxy results indeed in a rather weak stellar cusp, consistent with the observations. It appears that it is the first time that theory and observations are reaching convergence on the question of the stellar cusp. The fact that we can be sure now that there is a power-law cusp around Sagittarius A* also implies that the apparent deficit of giants within the innermost few arcsec of the central black hole indicates that the latter do not trace the overall cluster structure. Either they do not have the same age structure as the fainter stars or some process - such as a destruction of their envelopes via interactions with a fragmenting gaseous disc (the idea of Amaro-Seoane & Chen 2014) - has altered their apparent distribution.

The existence of a stellar cusp at the heart of the Milky Way implies that density cusps can also exist in many other galactic nuclei, especially smaller nuclei with relaxation times less than a Hubble time. This is of importance for gravitational wave astronomy because this means that EMRIs may be observed with significant frequency.

Acknowledgements. The research leading to these results has received funding from the European Research Council under the European Union's Seventh Framework Programme (FP7/2007-2013) / ERC grant agreement n° [614922]. PAS acknowledges support from the Ramón y Cajal Programme of the Ministry of Education and Science of Spain.

References

Aarseth, S. J. 1999, The Publications of the Astronomical Society of the Pacific, 111, 1333
Alexander, T. 1999, 527, 835
Alexander, T. & Hopman, C. 2009, 697, 1861
Amaro-Seoane, P. 2012, ArXiv e-prints [arXiv:1205.5240]
Amaro-Seoane, P., Aoudia, S., Babak, S., et al. 2013, GW Notes, Vol. 6, p. 4-110, 6, 4
Amaro-Seoane, P., Aoudia, S., Babak, S., et al. 2012, Classical and Quantum Gravity, 29, 124016
Amaro-Seoane, P. & Chen, X. 2014, 781, L18
Amaro-Seoane, P., Freitag, M., & Spurzem, R. 2004 [astro-ph/0401163]
Amaro-Seoane, P., Gair, J. R., Freitag, M., et al. 2007, Classical and Quantum Gravity, 24, 113
Amaro-Seoane, P., Gair, J. R., Pound, A., Hughes, S. A., & Sopuerta, C. F. 2015, Journal of Physics Conference Series, 610, 012002
Amaro-Seoane, P. & Preto, M. 2011, Classical and Quantum Gravity, 28, 094017
Antonini, F., Capuzzo-Dolcetta, R., Mastrobuono-Battisti, A., & Merritt, D. 2012, 750, 111
Bahcall, J. N. & Wolf, R. A. 1976, ApJ, 209, 214
Bahcall, J. N. & Wolf, R. A. 1977, 216, 883
Bailey, V. C. & Davies, M. B. 1999, 308, 257
Baumgardt, H., Gualandris, A., & Portegies Zwart, S. 2006, 372, 174
Baumgardt, H., Makino, J., & Ebisuzaki, T. 2004, ApJ, 613, 1143
Baumgardt, H., Makino, J., & Hut, P. 2005, ApJ, 620, 238
Boehle, A., Ghez, A. M., Schödel, R., et al. 2016, ApJ, 830, 17
Bressan, A., Marigo, P., Girardi, L., et al. 2012, MNRAS, 427, 127
Buchholz, R. M., Schödel, R., & Eckart, A. 2009, å, 499, 483
Chen, X. & Liu, F. K. 2013, 762, 95
Dale, J. E., Davies, M. B., Church, R. P., & Freitag, M. 2009, 393, 1016
Davies, M. B., Blackwell, R., Bailey, V. C., & Sigurdsson, S. 1998, 301, 745
Do, T., Ghez, A. M., Morris, M. R., et al. 2009, 703, 1323
Do, T., Kerzendorf, W., Winsor, N., et al. 2015, ApJ, 809, 143
Ernst, A., Just, A., & Spurzem, R. 2009, 399, 141
Freitag, M., Amaro-Seoane, P., & Kalogera, V. 2006, 649, 91
Gallego Cano, E., Schödel, R., H., D., et al. 2017
Genzel, R., Eisenhauer, F., & Gillessen, S. 2010, Reviews of Modern Physics, 82, 3121
Genzel, R., Thatte, N., Krabbe, A., Kroker, H., & Tacconi-Garman, L. E. 1996, 472, 153
Gong, X., Lau, Y.-K., Xu, S., et al. 2015, Journal of Physics Conference Series, 610, 012011
Gualandris, A. & Merritt, D. 2009, ApJ, 705, 361
Gualandris, A. & Merritt, D. 2012, 744, 74
Hansen, B. M. S. & Milosavljević, M. 2003, 593, L77
Kieffer, T. F. & Bogdanović, T. 2016, 823, 155
Kim, S. S. & Morris, M. 2003, 597, 312
King, I. R. 1966, 71, 64
Kroupa, P. 2001, 322, 231
Löckmann, U. & Baumgardt, H. 2008, 384, 323
Löckmann, U., Baumgardt, H., & Kroupa, P. 2010, MNRAS, 402, 519
Matsubayashi, T., Makino, J., & Ebisuzaki, T. 2007, 656, 879
Merritt, D. 2010, 718, 739
Nitadori, K. & Aarseth, S. J. 2012, MNRAS, 424, 545
Pfuhl, O., Fritz, T. K., Zilka, M., et al. 2011, ApJ, 741, 108
Pfuhl, O., Gillessen, S., Eisenhauer, F., et al. 2015, 798, 111
Portegies Zwart, S. F., Baumgardt, H., McMillan, S. L. W., et al. 2006, 641, 319
Preto, M. & Amaro-Seoane, P. 2010a, 708, L42
Preto, M. & Amaro-Seoane, P. 2010b, 708, L42
Ryde, N. & Schultheis, M. 2015, A&A, 573, A14
Schödel, R., Eckart, A., Alexander, T., et al. 2007, 469, 125
Schödel, R., Feldmeier, A., Neumayer, N., Meyer, L., & Yelda, S. 2014, Classical and Quantum Gravity, 31, 244007
Schödel, R., Gallego Cano, E., H., D., et al. 2017
Schödel, R., Najarro, F., Muzic, K., & Eckart, A. 2010, A&A, 511, A18
Spitzer, L. 1987, Dynamical evolution of globular clusters (Princeton, NJ, Princeton University Press, 1987, 191 p.)
Yu, Q. & Tremaine, S. 2003, 599, 1129